Physics Letters A 376 (2012) 978–981

Contents lists available at SciVerse ScienceDirect

Physics Letters A

www.elsevier.com/locate/pla

Thermoelectric figure of merit in Ga-doped [0001] ZnO nanowires

Lihong Shi [a], Jie Chen [a], Gang Zhang [b,*], Baowen Li [a,c,1]

[a] Centre for Computational Science and Engineering and Department of Physics, National University of Singapore, 117546, Singapore
[b] Key Laboratory for the Physics and Chemistry of Nanodevices and Department of Electronics, Peking University, Beijing 100871, People's Republic of China
[c] NUS Graduate School for Integrative Sciences and Engineering (NGS), National University of Singapore, 117456, Singapore

ARTICLE INFO

Article history:
Received 22 September 2011
Received in revised form 10 December 2011
Accepted 27 December 2011
Available online 29 December 2011
Communicated by R. Wu

Keywords:
Thermoelectric figure of merit
ZnO nanowires

ABSTRACT

By using first-principles electronic structure calculation and Boltzmann transport equation, we investigate the impact of gallium (Ga) doping on the thermoelectric property of [0001] zinc oxide nanowires ($Zn_{1-x}Ga_xO$ NWs). Our results show that the thermoelectric performance of the $Zn_{1-x}Ga_xO$ NWs is strongly dependent on the Ga contents. The maximum achievable room temperature thermoelectric figure of merit in $Zn_{1-x}Ga_xO$ NW can be increased by a factor of 2.5 at Ga content of 0.04, compared with the *ZT* of pure ZnO NWs. This may open up ZnO NW arrays applications in possible thermoelectric energy generator and cooler.

Recently, zinc oxide (ZnO) nanowires (NWs) have shown promise for nanodevice applications. Through the coupling of piezoelectric and semiconducting properties of ZnO, nanoscale mechanical energy can be converted into electrical energy by using ZnO NW arrays. Moreover, compared to traditionally TiO_2 films, ZnO NW arrays are considered promising anode material for photovoltaic device because of the highly controllable single-crystalline morphology which provides direct electron transport pathway. In addition to piezoelectric [1] and optoelectronic applications [2–4], thermoelectric effect is also an important approach to the solution to the energy crisis by converting waste heat into electricity. The energy conversion efficiency of a thermoelectric material is described by the dimensionless figure of merit *ZT*, which is a function of Seebeck coefficient, electrical conductivity, absolute temperature and thermal conductivity. The study of the thermoelectric property of ZnO ceramics has been motivated by the reports of the improved electrical conductivity and reduced thermal conductivity by employing elements (Al, Ga, Mn) as dopants [5–7]. In the Al and Ga dually doped ZnO ceramics, *ZT* is about twice of that of pure ZnO, which can arrive 0.65 at 1247 K [5]. A natural question comes promptly: How to improve the thermoelectric property of ZnO NWs? Although some research works have been done on the electrical properties of ZnO NWs [8–11], very little attention has been paid to the thermoelectric properties of ZnO NWs [12]. In this Letter, we will study thermoelectric properties through first-principle calculation, 1D Boltzmann transport theory (BTE), and molecular dynamics simulations. In particular, we will explore the impacts of Ga doping on the thermoelectric performance of $Zn_{1-x}Ga_xO$ NWs.

We focus on $Zn_{1-x}Ga_xO$ NWs oriented along the [0001] direction, with hexagonal cross section enclosed by $(10\bar{1}0)$ facets, because this is the commonest used surface structure in experiments and simulations [8–10]. It has been demonstrated that with the NW diameter increases, the thermoelectric power factor decreases, while thermal conductivity increases, which results in the reduction in thermoelectric figure of merit [13]. Moreover, larger system size is challenge to current computational capability. As the main concern of this work is the impact of Ga doping on the thermoelectric property of $Zn_{1-x}Ga_xO$ NWs, only thin ZnO NWs with the diameter of about 0.7 nm are considered here. The atomic structure of $Zn_{1-x}Ga_xO$ NW is initially constructed from bulk wurtzite structure of ZnO solid. The Zn atoms are randomly substituted by Ga atoms and the geometry is relaxed to its closest minimum total energy. A supercell approach is adopted where each wire is periodically repeated along the growth direction. The size of the supercells in the transverse plane is large enough (> 15 Å from surface to surface). Two repeated units along the growth direction are required for $Zn_{1-x}Ga_xO$ NWs and the relaxed supercell length along the wire axis is about 10.4 Å [14]. The total atom number of pure ZnO NWs is 52, with 26 Zn atoms and 26 O atoms. In this Letter, the density functional theory (DFT) calculations are carried out by DMol^3 package [15]. The DFT calculations are performed by using generalized gradient approximation with the functional parameterized by Perdew, Burke, and Ernzerhof [16]. And the double-numerical-polarization basis set is employed. Self-consistent field calculations are done with a convergence criterion of 10^{-6} hartree on the total energy. The Brillouin zone integration is performed using a $1 \times 1 \times 16$ Monkhorst–Pack *k*-point grid. All the structures are

* Corresponding author. Tel.: +86 10 62755317; fax: +86 10 62755317.
E-mail addresses: zhanggang@pku.edu.cn (G. Zhang), phylibw@nus.edu.sg (B. Li).
[1] Tel.: +65 6516 6864; fax: +65 6774 6756.

0375-9601/$ – see front matter
doi:10.1016/j.physleta.2011.12.040

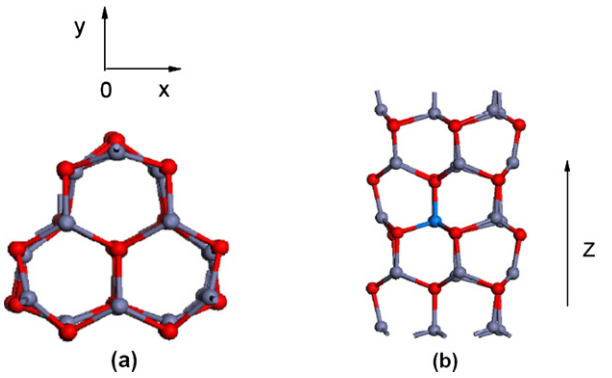

Fig. 1. The geometry of relaxed $Zn_{1-x}Ga_xO$ NWs for $x = 0.04$. (a) Top view and (b) side view. Ga, Zn and O atoms are represented in blue, gray and red, respectively. (For interpretation of the references to color in this figure legend, the reader is referred to the web version of this Letter.)

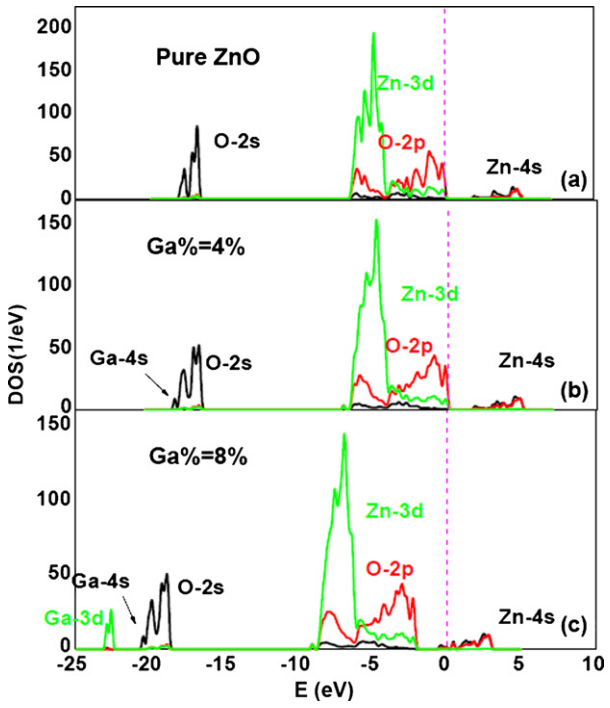

Fig. 2. The total DOS for $Zn_{1-x}Ga_xO$ NWs for (a) $x = 0$; (b) 0.04 and (c) 0.08. The Fermi energy is set to 0. The dashed magenta line is used to guide the eyes. (For interpretation of the references to color in this figure legend, the reader is referred to the web version of this Letter.)

fully optimized with a convergence criterion of 0.002 hartree/Å for the forces and 0.005 Å for the displacement. A real-space cut-off of 4.0 Å for the atom-centered basis set is chosen to increase computational efficiency while not significantly affecting the magnitude of inter-atomic forces or the total energies. The Gaussian smearing of electron density is applied with the energy range of 0.1 eV.

The electrical conductivity σ, the thermal conductivity due to electrons k_e, and the Seebeck coefficient S, are obtained from the electronic structure with the solution of one-dimensional Boltzmann transport equation as described in Refs. [13,17]. The electron relaxation time is an important factor for the electrical transport. In doped ZnO thin film, the scattering process is dominated by ionized dopant atoms and boundary. An analytical expression for the mobility of doped ZnO thin film, taking into account the non-parabolicity of the band edge, has been given by Ellmer and Mientus [18]. In doped ZnO nanowire, there is additional scattering mechanism from nanowire surface. However, as experimental mobility data for single crystalline ZnO nanowires are not available, here we use the experimental data of $Zn_{1-x}Ga_xO$ thin film [18,19] to calculate the carrier concentration dependent relaxation time, based on the assumption of a similar boundary scattering mechanism in thin film and nanowire. Only perfect NW is considered here, so there is no defect scattering. The carrier concentration is defined as: $n = \int_{-\infty}^{\infty} D(E-\mu) f(E-\mu)\, dE$, where $f(E)$ is the Fermi distribution function.

Fig. 1 shows the atomic structure for the $Zn_{1-x}Ga_xO$ NW for $x = 0.04$ with the replacement of one Zn atom in the supercell. $x = 0.08$ and 0.12 corresponds to two and three Zn atoms are substituted with Ga atoms, respectively. Fig. 2 shows the total density of states (DOS) of $Zn_{1-x}Ga_xO$ NWs. For pure ZnO NW ($x = 0$), the O 2s states are located around -18 eV, which have little interaction with the other valence band. The valence band consists of two main states, Zn 3d and O 2p orbitals. The Zn 4 s states dominate the conductance band. With the Ga content (x) increase, on the one hand, there is charge transfer from Zn 4 s states to O 2p states, thus results in the shift of the center of gravity of the DOS at the O sites towards the low energy regions and the Fermi energy level into the conduction band (see Fig. 2(c)), which indicates the n-type characteristics of $Zn_{1-x}Ga_xO$ wires. And on the other hand, the dopant states (Ga 4 s states and Ga 3d states), appear following the O 2 s states. Similar phenomena can be observed in Ga-doped bulk ZnO [20].

Fig. 3(a) shows the Ga content (x) dependent electronic band gap and carrier concentration. It is obvious that for each Ga content, the band gap values depend on the detailed atomic structures. In order to reduce the fluctuation, the results are averaged by over five realizations such as the case in $Si_{1-x}Ge_x$ NWs [17]. With Ga content (x) increase, the averaged band gap decreases. This is consistent with the experimental observed energy band gap in [21]. In the following calculation of the thermoelectric properties, the DOS of specific NW structure is used, which is most stable with the lowest total energy. The carrier concentration increases as the Ga content increase. With $x = 0.08$, the carrier concentration is about 6.0×10^{20} cm^{-3}, and $n = 2.0 \times 10^{21}$ cm^{-3} when $x = 0.12$. However, the maximum electron concentration can be achieved in ZnO NWs via doping method is in the order of 10^{20} cm^{-3} [22], thus the maximum Ga doped content (x) we consider in this Letter is 0.08. Fig. 3(b) shows the Ga content dependence of σ and S. σ increases and S decreases as the Ga content increases because there is more charge concentration. At low carrier concentration range, the Seebeck coefficient is about 400 μV/K, which is in good agreement with the experimental observation in Ref. [12]. Fig. 3(c) shows the power factor ($P = S^2\sigma$) versus the Ga content. There is an optimal Ga content ($x = 0.04$, $n = 1.0 \times 10^{17}$ cm^{-3}) yielding the maximum attainable value of power factor ($P_{\max} = 908$ μW/mK^2).

ZT is one of the central physical quantities that determine the efficiency of thermoelectric application. In the calculation of *ZT*, both electrons and phonons contribute to the total thermal conductivity. To calculate the phonon thermal conductivity of $Zn_{1-x}Ga_xO$ NW by using molecular dynamics simulations, the potential that describes the interactions between the atoms is needed. However, there is no consensus in the literature about the potential between Ga, O and Zn atoms. In the $Zn_{1-x}Ga_xO$ NW, compare to the original Zn atom, the doped Ga atom has different atomic mass and different interaction with the neighboring atoms. Through the investigation of thermal conductivity by using molecular dynamics simulation, it has been demonstrated that the difference in atomic mass has larger impact on thermal conductivity than the different interaction does [23]. Thus here we use the Buckingham potential [24] to describe the atomic interaction in $Zn_{1-x}Ga_xO$ NW, which includes anharmonicity to describe the phonon–phonon scattering process. In the molecular dynam-

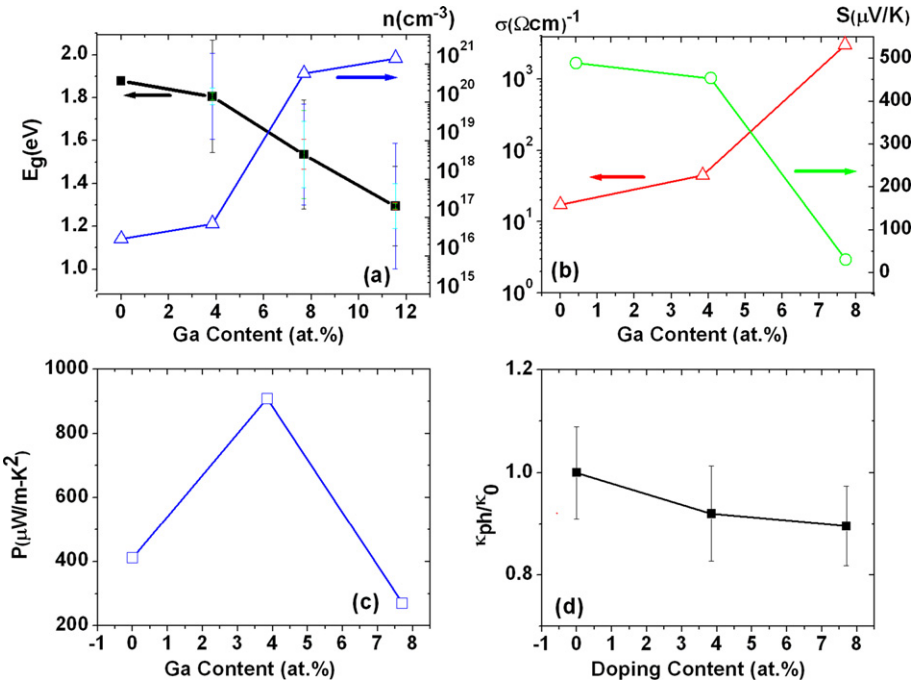

Fig. 3. (a) The averaged electronic band gap and carrier concentration versus Ga contents for $Zn_{1-x}Ga_xO$ NWs. (b) Electrical conductivity σ and Seebeck coefficient S versus Ga content x. (c) Power factor of $Zn_{1-x}Ga_xO$ NWs versus Ga contents. (d) Phonon thermal conductivity versus doping contents at room temperature. Here κ_0 is the thermal conductivity of pure ZnO NW.

ics simulation, there are 20 unit cells in the longitudinal direction which corresponds to a length of 10.4 nm, and the wire diameter is 0.7 nm, the same as that in the DFT calculation. In order to establish a temperature gradient along the NW longitudinal direction, the two ends of NWs are put into Nosé–Hoover heat bathes with different temperature. The simulations are performed long enough to allow the system to reach a non-equilibrium steady state. All results given in this Letter are obtained by averaging about 1×10^7 time steps, a time step is set as 0.8 fs. Free boundary condition is used to atoms on the outer surface of the NWs. The thermal conductivity is calculated from $\kappa = -J_L/\nabla T$, where the heat current J_L along the longitudinal direction is defined as the energy transported along the NW in unit time through the unit cross-section area, and ∇T is the temperature gradient.

Fig. 3(d) shows that the phonon thermal conductivity decreases as the Ga content increases. Compared to the 60% thermal conductivity reduction (with $x = 0.1$) in $Si_{1-x}Ge_x$ NW, the thermal conductivity reduction in $Zn_{1-x}Ga_xO$ NW is only about 10%, due to the small difference in atomic masses between Zn and Ga atoms [25].

Combined the calculations of the power factor and the phonon thermal conductivity, we show the Ga content dependent ZT in Fig. 4. The value of ZT firstly increases with the Ga content, reaches a maximum value at $x = 0.04$, which is 2.5 times larger than that of pure ZnO wires, and then decreases. This phenomenon can be explained as follows. ZT is contributed by both power factor and thermal conductivity. With Ga content increase, the power factor increases, reaches a maximum value at $x = 0.04$ and then decreases. The curve of the thermal conductivity decreases with the Ga content increases. Thus when $0 \leqslant x \leqslant 0.04$, ZT increases with the Ga content. However, when $0.04 \leqslant x \leqslant 0.08$, the reduction in the thermal conductivity cannot offset the reduction in the power factor, thus results in the decrease in ZT with the Ga content. It is worth to mention that the optimal carrier concentration yielding the maximum attainable value of ZT is 1.0×10^{17} cm^{-3}. This low carrier concentration suggests that the high thermoelectric performance of Ga-doped ZnO NW can be realized by using reliable fabrication technology. It is worth pointing that the optimal Ga content, 4% yielding a 2.5 times enhancement in ZT is an approximated value due to the limited supercell size. To get a more accurate optimal Ga content, larger supercell size is required, which is challenge to current computational capability. However, our results demonstrate that at least a 2.5 times enhancement in ZT can be achieved under a reliable doping concentration. As the Seebeck coefficient is similar to the value of pure ZnO NW, it is obvious that the enhancement in ZT is mainly due to the increase in electrical conductivity and reduction in thermal conductivity.

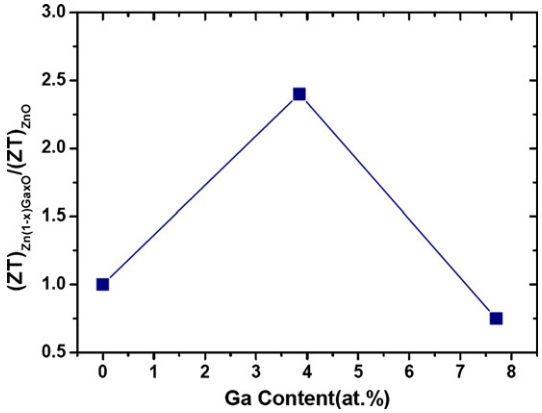

Fig. 4. $ZT_{Zn_{1-x}Ga_xO}/ZT_{ZnO}$ versus the Ga content for $Zn_{1-x}Ga_xO$ NW. The solid line is used to guide the eyes.

In summary, we have investigated the Ga content dependent thermoelectric properties in $Zn_{1-x}Ga_xO$ nanowires. It is found that the thermoelectric performance is strongly dependent on the Ga content. The Ga doping has reduced the thermal conductivity of ZnO NW, down to less than 90% at Ga content of 0.08. The maximum attainable ZT corresponds to an optimal Ga content of $x = 0.04$, which is 2.5 times of that of the pure ZnO wires. Our work open up possible ZnO NW arrays applications in thermoelectric energy generation and refrigeration.

Acknowledgement

The work has been supported by an NUS Grant R-144-000-285-646. The work has been also supported in part by a grant from the Asian Office of Aerospace Research and Development of the U.S. Air Force (AOARD-114018). G.Z. was supported by the Ministry of Science and Technology of China (Grant No. 2011CB933001).

References

[1] Z.L. Wang, J.H. Song, Science 312 (2006) 242.
[2] M.H. Huang, S. Mao, H. Feick, H.Q. Yan, Y.Y. Wu, H. Kind, E. Weber, R. Russo, P.D. Yang, Science 292 (2001) 1897.
[3] H. Cao, J.Y. Xu, D.Z. Zhang, S.-H. Chang, S.T. Ho, E.W. Seelig, X. Liu, R.P.H. Chang, Phys. Rev. Lett. 84 (2000) 5584.
[4] D.M. Bagnall, et al., Appl. Phys. Lett. 70 (1997) 2230.
[5] M. Ohtaki, K. Araki, K. Yamamoto, J. Elec. Mater. 38 (2009) 1234.
[6] E. Guilmeau, A. Maignan, C. Martin, J. Elec. Mater. 38 (2009) 1104.
[7] C.K. Ghosh, S. Das, K.K. Chattopadhyay, Phys. B 399 (2007) 38.
[8] H. Xu, A.L. Rosa, T. Frauenheim, R.Q. Zhang, S.T. Lee, Appl. Phys. Lett. 91 (2007) 031914.
[9] Y. Zhang, Y.H. Wen, J.C. Zheng, Z.Z. Zhu, Appl. Phys. Lett. 94 (2009) 113114.
[10] H. Xu, W. Fan, A.L. Rosa, R.Q. Zhang, T. Frauenheim, Phys. Rev. B 79 (2009) 073402.
[11] W. Fan, H. Xu, A.L. Posa, T. Frauenheim, R.Q. Zhang, Phys. Rev. B 76 (2009) 073302.
[12] C.H. Lee, G.C. Yi, Y.M. Zuev, P. Kim, Appl. Phys. Lett. 94 (2009) 022106.
[13] L.H. Shi, D.L. Yao, G. Zhang, B. Li, Appl. Phys. Lett. 95 (2009) 063102.
[14] B.L. Wang, J.J. Zhao, J.M. Jia, D.N. Shi, J.G. Wan, G.H. Wang, Appl. Phys. Lett. 93 (2008) 021918.
[15] B. Delley, J. Chem. Phys. 92 (1990) 508.
[16] J.P. Perdew, K. Burke, M. Ernzerhof, Phys. Rev. Lett. 77 (1996) 3865.
[17] L.H. Shi, D.L. Yao, G. Zhang, B. Li, Appl. Phys. Lett. 96 (2010) 173108.
[18] K. Ellmer, R. Mientus, Thin Solid Films 516 (2008) 4620.
[19] R.P. Wang, A.W. Sleight, D. Cleary, Chem. Mater. 8 (1996) 433.
[20] C.Y. Ren, S.H. Chiou, C.S. Hsue, Phys. B 349 (2004) 136.
[21] M. Snure, A. Tiwari, J. Appl. Phys. 101 (2007) 124912.
[22] D.R. Khanal, J.W.L. Yim, W. Waluwicz, J. Wu, Nano Lett. 7 (2007) 1186.
[23] J. Chen, G. Zhang, B. Li, Appl. Phys. Lett. 95 (2009) 073117.
[24] D. Wolf, P. Keblinski, S.R. Phillpot, J. Eggebrecht, J. Chem. Phys. 110 (1999) 8254.
[25] N. Yang, G. Zhang, B. Li, Nano Lett. 8 (2008) 276.